Complex Dynamics of Spring-Block Earthquake Model Under Periodic Parameter Perturbations

Srđan Kostić[1]
Department of Geology,
University of Belgrade Faculty
of Mining and Geology,
Đušina 7,
Belgrade 11000 Serbia
e-mail: srdjan.kostic@rgf.bg.ac.rs

Nebojša Vasović
Department of Applied Mathematics,
University of Belgrade Faculty
of Mining and Geology,
Đušina 7,
Belgrade 11000 Serbia
e-mail: nebojsa.vasovic@rgf.bg.ac.rs

Igor Franović
Department of Theoretical Mechanics,
Statistical Physics, and Electrodynamics,
University of Belgrade Faculty of Physics,
Studentski Trg 12,
Belgrade 11000 Serbia
e-mal: igor.franovic@gmail.com

Kristina Todorović
Department of Physics and Mathematics,
University of Belgrade Faculty of Pharmacy,
Vojvode Stepe 450,
Belgrade 11000 Serbia
e-mail: kisi@pharmacy.bg.ac.rs

A simple model of earthquake nucleation that may account for the onset of chaotic dynamics is proposed and analyzed. It represents a generalization of the Burridge–Knopoff single-block model with Dieterich–Ruina's rate- and state-dependent friction law. It is demonstrated that deterministic chaos may emerge when some of the parameters are assumed to undergo small oscillations about their equilibrium values. Implementing the standard numerical methods from the theory of dynamical systems, the analysis is carried out for the cases having one or two periodically variable parameters, such that the appropriate bifurcation diagrams, phase portraits, power spectra, and the Lyapunov exponents are obtained. The results of analysis indicate two different scenarios to chaos. On one side, the Ruelle–Takens–Newhouse route to chaos is observed for the cases of limit amplitude perturbations. On the other side, when the angular frequency is assumed constant for the value near the periodic motion of the block in an unperturbed case, variation of oscillation amplitudes probably gives rise to global bifurcations, with immediate occurrence of chaotic behavior. Further analysis shows that chaotic behavior emerges only for small oscillation frequencies and higher perturbation amplitudes when two perturbed parameters are brought into play. If higher oscillation frequencies are assumed, no bifurcation occurs, and the system under study exhibits only the periodic motion. In contrast to the previous research, the onset of chaos is observed for much smaller values of the stress ratio parameter. In other words, even the relatively small perturbations of the control parameters could lead to deterministic chaos and, thus, to instabilities and earthquakes. [DOI: 10.1115/1.4026259]

Keywords: spring-block model, coupled oscillations, spring constant, stress ratio, deterministic chaos

1 Introduction

Understanding the development and initial stages of an earthquake rupture is a major goal of earthquake science. Some researchers suggest that the nucleation process, specifically the size of the nucleation zone, is related to the ultimate size of the resulting earthquake [1–3], while others support the view that the size of the nucleation zone is unrelated to the final magnitude of an earthquake [4,5]. However, the influence of the nucleation mechanism on the final impact of an earthquake certainly exists, so the modeling of this phenomenon could lead to new insights on the nature of earthquakes. A common approach in the description of seismic sources is their approximation by a model of equivalent forces that correspond to the linear wave equations, neglecting nonlinear effects in the source area [6–8]. Equivalent forces are defined as the forces that produce displacements at a given point that are identical to those from the real forces acting at the source. Nevertheless, this body-force equivalent is a formal concept and it is necessary to relate its characteristics to the real earthquake source. Today, it is commonly accepted that vast majority of shallow tectonic earthquakes arise from faulting instabilities [9]. However, since the earthquake origin is not accessible to direct observation, the research in this area is conducted either by studying the recorded time series, propagation of seismic waves through the Earth's interior, or by simulating the earthquakes in laboratory conditions. In this paper, we succeed the suggestion of Brace and Byerlee [10], that stick-slip occurring in laboratory experiments on rock friction may be significant under shallow crustal conditions and that it can be regarded as a possible source of earthquakes.

Following the idea of Brace and Byerlee [10], Burridge and Knopoff [11] proposed a spring-block model, which is today recognized as a common model for the earthquake nucleation mechanism [12–14]. In the present paper, the Burridge–Knopoff (BK) model consists of only one block (Fig. 1), attached through a harmonic spring to a driving plate, which causes the block to move in a stick-slip fashion along the rough surface of the lower plate [15,16]. In the context of seismology, this spring-block model can be understood as a representation for earthquake motion [17–21].

The main nonlinearity of this system comes from the friction between the block and the rough surface of the lower plate. Concerning this, some specific constitutive laws for rock friction have been developed based on laboratory studies. These laws have been successfully used to explain various aspects of stable and unstable sliding between elastic solids as observed in the laboratory [22,23]. In the present paper, we use the Dieterich–Ruina rate- and state-dependent friction law [24].

Though the simulations of the BK model have led to much insight, one should still be mindful about its character, which is, especially in the elementary configuration, closer to that of a toy model than the realistic representation of the fault dynamics. The model's realism has been contested for a number of reasons that generally fall into two categories, one related to the basic setup and the other concerned with the friction laws applied [25]. With respect to the former, some of the strongest criticisms refer to a lack of mechanisms by which the seismic energy is radiated or

[1]Corresponding author.

Contributed by the Design Engineering Division of ASME for publication in the Journal of Computational and Nonlinear Dynamics. Manuscript received June 10, 2013; final manuscript received December 11, 2013; published online March 13, 2014. Assoc. Editor: Ahmet S. Yigit.

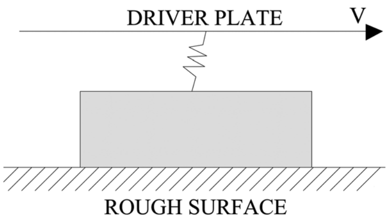

Fig. 1 The Burridge–Knopoff block and spring model, represented by a slider coupled through a spring to a loader plate, which moves with velocity *V*

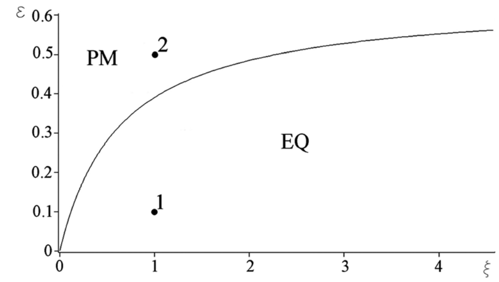

Fig. 3 Attractors of the system (3) (or (4) with $\delta_i = 0$) in parameter plane ε-ξ. The remaining parameters are held fixed at values admitting the equilibrium point, as in Fig. 2 Corresponding time series and phase portraits for points 1 and 2 are shown in Fig. 4 EQ and PM are abbreviations for equilibrium state and periodic motion, respectively.

dissipated. Apart from that, attention has also been directed to the absence of the long-range stress transfer and the possibility that the displayed complexity of the small events may be an artifact related to the lack of the continuum limit. As for the Dieterich–Ruina friction law, a drawback lies in that it is valid only for aseismic slip velocities but fails within the range of the seismic ones [26]. The intention here is not to address the specific issues outlined above but rather to point out how there may be some effects and influences whose inclusion into the original model may prove beneficial in qualitative terms. The latter expectation also draws on some of the advantages of the BK model, one of them being that the impact of the introduced variables and parameters is easily tractable. Proceeding in this spirit, the aim is to isolate some potentially novel mechanisms that may contribute to the emergence of chaotic dynamics in the monoblock setup. In particular, we propose a mechanism related to some external effects, like dynamic triggering from distant earthquake or vibrations caused by some artificial source.

In the present paper, we analyze a system of equations proposed by Madariaga, already used in Refs. [20,27], under the assumption that nondimensional stress change ratio and spring constant exhibit simple sinusoidal time dependence. The aim of the research is to show whether this kind of perturbation would generate complex dynamics, giving rise to the onset of deterministic chaos. Moreover, our idea was to determine whether the onset of chaos is also possible in the single-block model, only by coupling two sinusoidal oscillators, which is a common theoretical approach frequently used in the area of nonlinear dynamics.

It has to be emphasized that even though seismic waves do not generate such idealistic perturbations, they are of interest because of their simple shape and because a real wave pattern results in a superposition of such periodic waves. These idealistic perturbations also set the basis for a more complex periodic perturbation in a form of a sine wave scaled by a Gaussian pulse [28]. Similar research was already performed by Perfettini et al. [29], except that they assumed a simplified pulselike stress change. Also, this kind of analysis with sinusoidal parameter perturbations was previously applied in the area of immunology, where periodic variation of a system's parameters is ascribed to some external perturbations [30].

The purpose of this paper is to provide a minimal, yet sufficient, model of fault dynamics that may give rise to chaotic behavior. One may appreciate the simplicity tied to such an approach, given that a couple of possible mechanisms are laid out that are easy to incorporate as subtle modifications to the original Burridge–Knopoff model with the well-known Dieterich–Ruina's rate- and state-dependent friction law. An important point is that the considered setups do not presuppose a compound fault structure but rather build on the simplest possible monoblock arrangement. It turns out that the inclusion of minor perturbations to the system parameters may be all that it takes for the system to exhibit robust chaotic dynamics. One cannot rule out the possibility that similar mechanisms operating alone or in synergy with the ones stated above may partially contribute to the occurrence of chaotic dynamics on real faults.

The scheme of the paper is as follows. In Sec. 2, we describe the original model in detail, while the modified model is presented in Sec. 3. Section 4 provides the main results, with detailed analysis of the system's dynamics when either one or both parameters are perturbed. The obtained complex dynamical behavior is confirmed by calculating the Fourier power spectrum and the largest Lyapunov exponent. Concluding remarks are given in Sec. 5 with suggestions for further research.

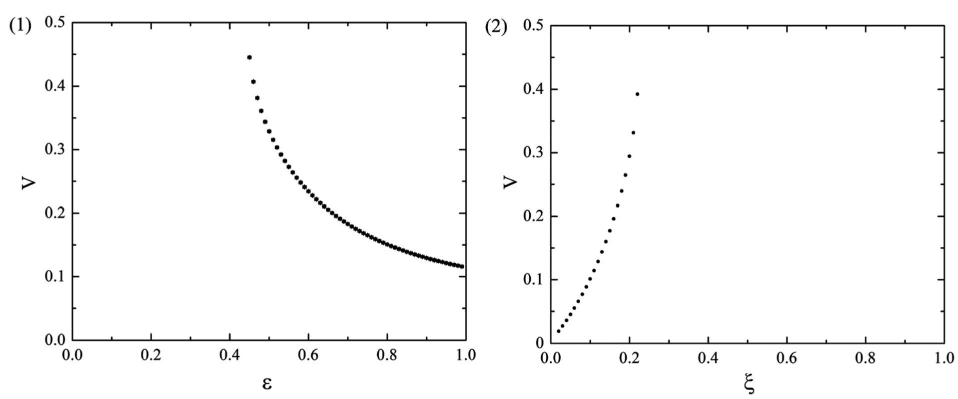

Fig. 2 Bifurcations of the system (2) (or (3) if $\delta_i = 0$ is set) under the variation of one of the parameters ε (*1*) and ξ (*2*). Orbital diagram is constructed for the section with plane $\theta = 1$, and calculation step 0.01, showing the asymptotic dynamics after 8×10^6 time units. At each instance, the parameters held constant are awarded values that admit the equilibrium point, $\varepsilon = 0.2$, $\xi = 0.6$, and $\gamma = 0.8$.

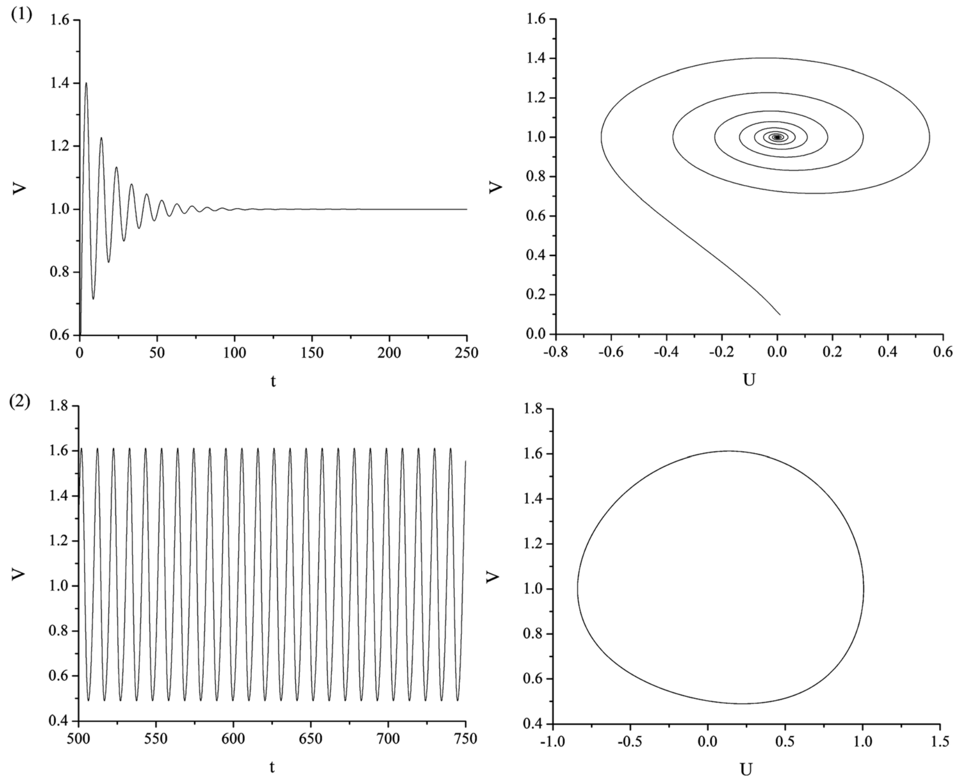

Fig. 4 Temporal evolution of variable V and the appropriate phase portraits for: (*1*) $\varepsilon = 0.1$, $\xi = 1.0$, and $\gamma = 0.8$ (equilibrium state); (*2*) $\varepsilon = 0.5$, $\xi = 1$, and $\gamma = 0.8$ (periodic motion)

2 Background of the Original Model

The present analysis on complex dynamics of a spring-block model is based on the system of equations proposed by Madariaga [20]. These equations of motion coupled with the Dieterich–Ruina rate- and state-dependent friction law are originally given by

$$\begin{aligned} \dot{\theta} &= -\left(\frac{V}{L}\right)\left(\theta + B\log\left(\frac{V}{V_0}\right)\right) \\ \dot{U} &= V - V_0 \\ \dot{V} &= \left(-\frac{1}{M}\right)\left(kU + \theta + A\log\left(\frac{V}{V_0}\right)\right) \end{aligned} \tag{1}$$

where parameter M is the mass of the block and the spring stiffness k corresponds to the linear elastic properties of the rock mass surrounding the fault [18]. According to Dieterich and Kilgore [31] the parameter L corresponds to the critical sliding distance necessary to replace the population of asperity contacts. The parameters A and B are empirical constants, which depend on material properties. According to Ref. [32], parameter A measures the direct velocity dependence ("direct effect") while $(A-B)$ is a measure of the steady-state velocity dependence. For convenience,

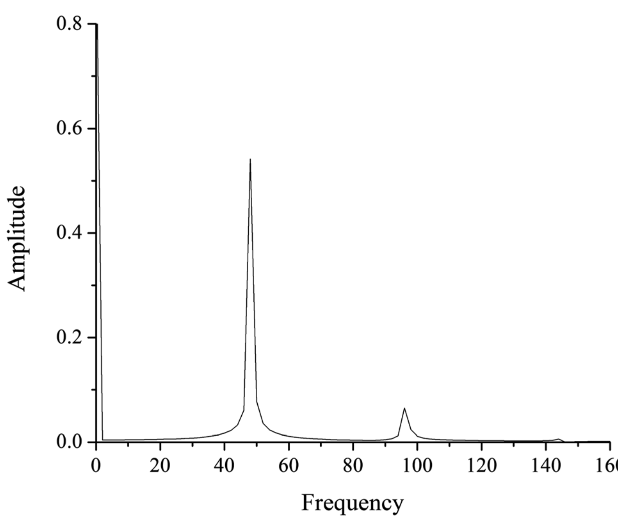

Fig. 5 Single peak in power spectrum indicates the oscillatory behavior of the model. Parameter values are the same as in Fig. 4(*2*).

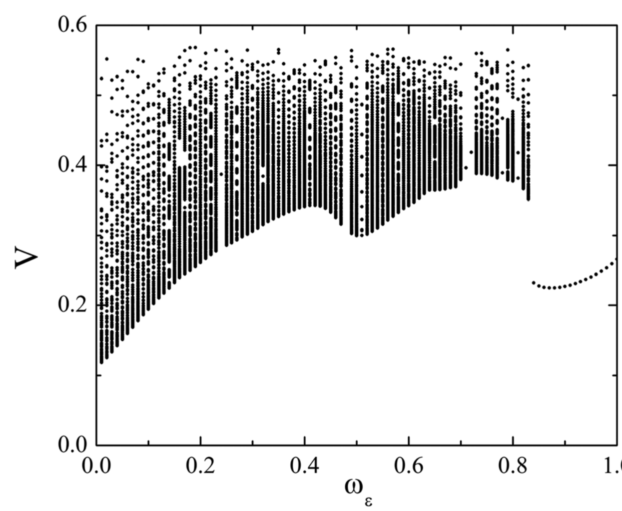

Fig. 6 Bifurcations of the system (3) under the variation of the parameter ε. Orbital diagram is constructed for the section with plane $\theta = 1$, and calculation step $\omega_\varepsilon = 0.01$, showing the asymptotic dynamics after 8×10^6 time units. At each instance, the parameters held constant are awarded the values near the equilibrium point but admitting the limit cycle, $\varepsilon = 0.4$ ($\delta_\varepsilon = 0.4$), $\xi = 0.5$, and $\gamma = 0.8$. Corresponding time series and phase portraits for periodic and chaotic motion are shown in Fig. 7.

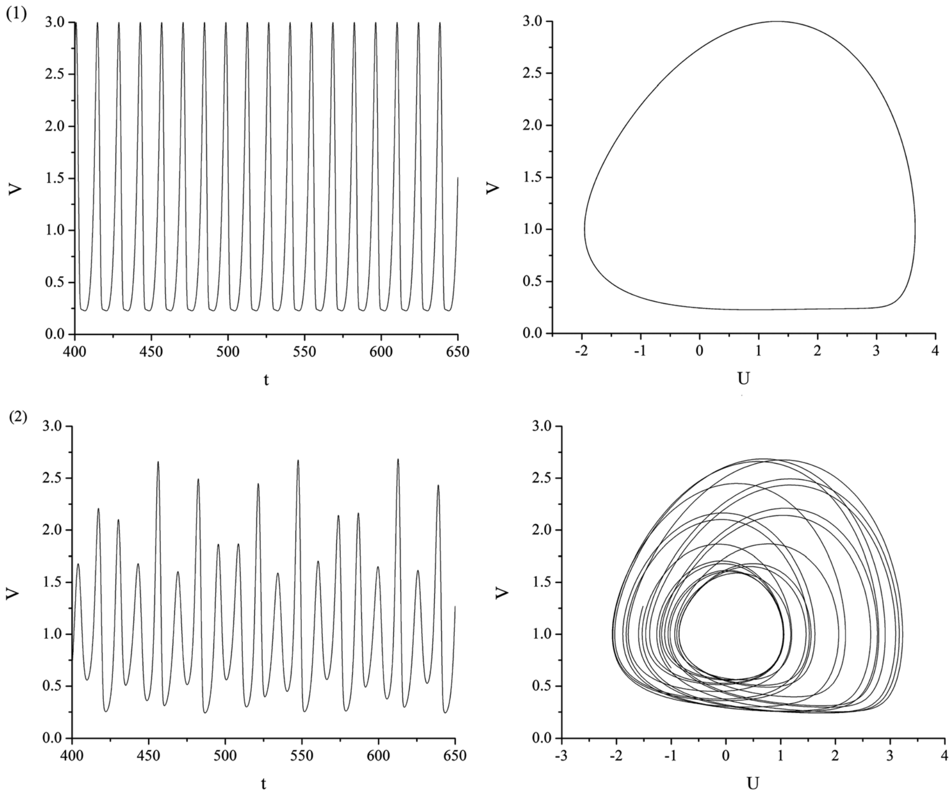

Fig. 7 Temporal evolution of variable V and the appropriate phase portraits for: (*1*) $\omega_\varepsilon = 0.9$ (periodic motion); (*2*) $\omega_\varepsilon = 0.2$ (deterministic chaos). At each instance, the parameters held constant are awarded the values near the equilibrium point, but admitting the limit cycle, $\varepsilon = 0.4$ ($\delta_\varepsilon = 0.4$), $\xi = 0.5$, and $\gamma = 0.8$.

system (2) is nondimensionalized by defining the new variables θ', V', U', and t' in the following way: $\theta = A\theta'$, $V = V_0 V'$, $U = LU'$, $t = (L/V_0)t'$, after which we return to the use of θ, V, U, and t. This nondimensionalization puts the system into the following form

$$\begin{aligned} \dot{\theta} &= -V(\theta + (1+\varepsilon)\log(V)) \\ \dot{U} &= V - 1 \\ \dot{V} &= -\gamma^2[U + (1/\xi)(\theta + \log(V))] \end{aligned} \tag{2}$$

where $\varepsilon = (B-A)/A$ measures the sensitivity of the velocity relaxation, $\xi = (kL)/A$ is the nondimensional spring constant, and $\gamma = (k/M)^{1/2}(L/V_0)$ is the nondimensional frequency [20].

3 Extended Model With Periodically Perturbed Parameters

In the present paper, the dynamics of a single-block model are analyzed by assuming the time-dependent character of ε and ξ in the following way:

$$\begin{aligned} \dot{\theta} &= -V[\theta + (1+\varepsilon(t))\log V] \\ \dot{U} &= V - 1 \\ \dot{V} &= -\gamma^2[U + (1/\xi(t))(\theta + \log V)] \end{aligned} \tag{3}$$

where $\varepsilon(t)$ and $\xi(t)$ are positive periodic functions of time:

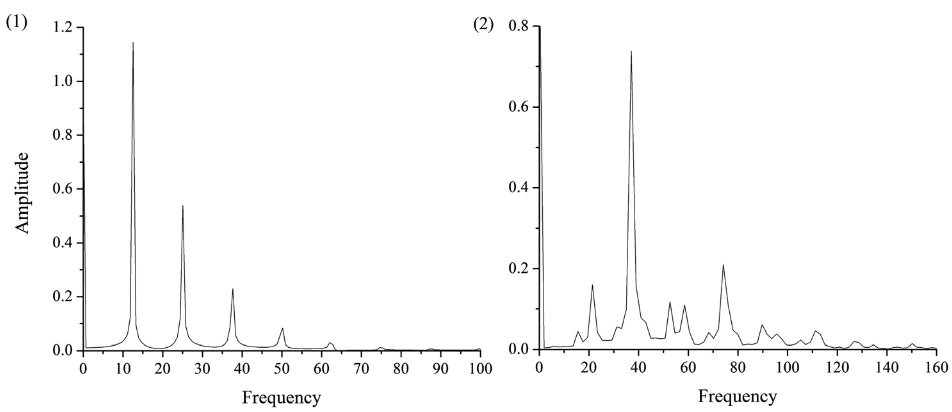

Fig. 8 (*1*) Fourier power spectrum of periodic motion (first peak is for fundamental frequency, other peaks represent harmonics); (*2*) the broadband noise in the Fourier power spectrum indicates the onset of deterministic chaos. Parameter values are the same as in Figs. 7(*1*) and 7(*2*), respectively.

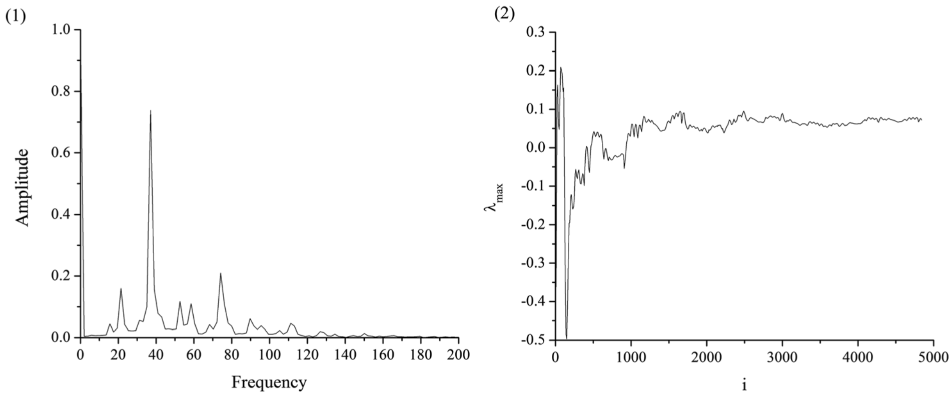

Fig. 9 Maximal Lyapunov exponent converges well to $\lambda_{max} = 0.072$, confirming the onset of deterministic chaos. The parameter values are identical to those in Fig. 7(*2*).

$$\varepsilon(t) = \varepsilon + \delta_\varepsilon \sin(\omega_\varepsilon t)$$
$$\xi(t) = \xi + \delta_\xi \sin(\omega_\xi t) \tag{4}$$

such that δ_ε, δ_ξ, ω_ε, and ω_ξ represent the constant oscillation amplitudes and the angular frequencies, respectively. The former satisfy the constraint $\delta_\varepsilon \leq \varepsilon$, $\delta_\xi \leq \xi$, which ensures the model's consistency as it confines each perturbation term to an appropriate range of values. The introduced modification addresses the issue of the system's response to an external perturbation, this aimed at showing that even the small-amplitude influences are sufficient to profoundly change the original behavior, leading to the onset of chaos. Within this framework, the external perturbations are incorporated implicitly by assuming that they induce small oscillations near the equilibrium values of some of the system parameters but admitting the periodic motion. Such persistent time-dependent perturbations may be attributed to the earthquakes that arise from slow rupture along the faults or to some nonnatural source of vibrations, on one side [33], or Earth tides and reservoir effects, on the other side [34]. However, note that the persistence of perturbations should be assessed in relative terms, meaning that even the impact of transient influences whose oscillation period is much shorter than the time they act on the system may still qualify for the provided description. In this context, one recalls the dynamical triggering models, which concern the possibility of earthquakes caused by the passage of seismic waves from the mainshock on some distant fault [35,36]. In particular, it has been proposed that the stress pulse emitted by the mainshock may increase another fault's slip speed or enhance triggering by reducing the associated state variable.

4 Numerical Analysis

The system (3) has only one stationary solution $(\theta,u,v) = (0,0,1)$, which corresponds to steady sliding. We shall proceed in the standard way to determine and analyze the dynamics of Eq. (3) around a stationary solution (0,0,1).

Let us first analyze the dynamics of the system (3) under the perturbation of one or two parameters, while the remaining ones are held fixed at values admitting the equilibrium point. To provide a point of reference, we first present the results on the stability of the equilibrium point for the autonomous system (2) if one of the parameters ε and ξ is varied, viz. Fig. 2.

In order to gain insight on how the interplay between the parameters affects the behavior of the original system (2), we further plot the attractors in the (ε, ξ) parameter plane, which is obtained analytically (Fig. 3). The corresponding diagrams for the other pairs of parameters are qualitatively similar. Corresponding time series and phase portraits for points 1 and 2 (in Fig. 3) are shown in Fig. 4. One learns that the variation of each of the parameters ε or ξ leads the system through the supercritical Hopf bifurcation, such that the equilibrium point goes unstable and a new stable limit cycle is created.

Periodic motion of the block is confirmed by calculating the Fourier power spectrum (Fig. 5).

As stated earlier, the main goal of the analysis is to examine whether some sinusoidal perturbations acting in the system may change its underlying dynamics, giving rise to the chaotic solutions. The perturbations are introduced in an implicit fashion, assuming that they induce oscillations of the system parameters near their equilibrium values before and after the bifurcation occurs in the original system (2) (Fig. 3). Our strategy consists of varying the parameters in the vicinity of their respective equilibrium values, verifying if the periodic perturbation of a certain amplitude and frequency can elicit the chaotic behavior in the system, whereas the perturbation amplitudes have to comply with the elementary constraint $\delta_\varepsilon \leq \varepsilon$ and $\delta_\xi \leq \xi$, the corresponding frequencies can assume a broader range of values.

The systematic exploration along these lines reveals the following results. First we address the issue of what occurs if only a single parameter, ε or ξ, undergoes periodic oscillations, while the other parameter is fixed. Note that the chosen parameter values would lead to the limit cycle in the unperturbed system (2). We start by changing the angular frequency of periodic oscillations of parameter ε, for the fixed upper limit value of amplitude

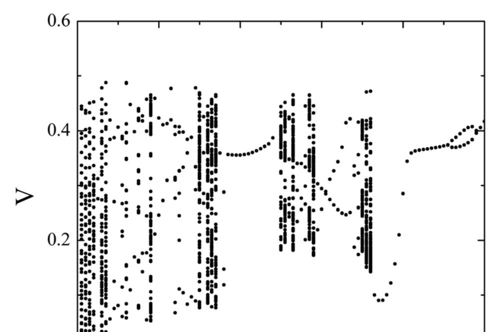

Fig. 10 Bifurcations of the system (3) under the variation of the parameter ξ. Orbital diagram is constructed for the section with plane $\theta = 1$, and calculation step $\omega_\xi = 0.01$, showing the asymptotic dynamics after 4×10^6 time units. At each instance, the parameters held constant are awarded values near the equilibrium point, but admitting the limit cycle, $\varepsilon = 0.4$, $\xi = 0.5$ ($\delta_\xi = 0.4$), and $\gamma = 0.8$. Corresponding time series and phase portraits for quasi-periodic motion are shown in Fig. 11.

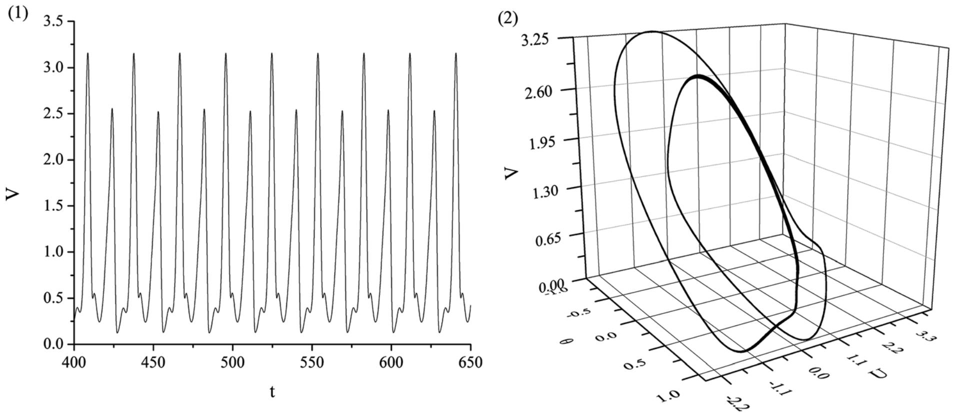

Fig. 11 Temporal evolution of variable *V* (*1*) and the appropriate phase portrait (*2*) for $\omega_\xi = 0.65$ (quasi-periodic motion). At each instance, the parameters held constant are awarded the values near the equilibrium point, but admitting the limit cycle, $\varepsilon = 0.4$ ($\delta_\varepsilon = 0.4$), $\xi = 0.5$, and $\gamma = 0.8$.

($\delta_\varepsilon = 0.4$). It turns out that as the parameter ω_ε takes smaller values at each step in the range [0,1], a transition from periodic motion to deterministic chaos is observed, with periodic and quasi-periodic windows interspersed between chaotic clouds of dots (Fig. 6). Note that in all of the examined cases trajectory intersects Poincare surface in only one direction. The typical time series and phase portraits for the corresponding time series are displayed in Fig. 7.

The transition to chaos is verified by calculating the Fourier power spectra for the time series presented in Fig. 7, with the results displayed in Fig. 8. The first maximal peak for fundamental frequency and several smaller peaks for harmonics (as integer multiples of the fundamental frequency) in Fig. 8(*1*) imply the periodic evolution of the system. The broadband noise in Fig. 8(*2*) suggests the emergence of a strange attractor. Maximal Lyapunov exponent, which is determined using the method of Wolf et al. [37] converges well to a positive value ($\lambda_{\max} \approx 0.072$), indicating the onset of deterministic chaos (Fig. 9).

The analysis of the system's dynamics when the perturbation of the parameter ξ (ω_ξ) is assumed (also for the fixed upper value of amplitude, $\delta_\xi = 0.4$) indicates a more complex picture, with successive transition from periodic and quasi-periodic motion to deterministic chaos, interspersed with periodic and quasi-periodic windows (Fig. 10). The corresponding time series and phase portrait for quasi-periodic motion are shown in Fig. 11.

The quasi-periodic motion is further verified by several incommensurate frequencies in Fourier power spectra (Fig. 12) for the time series presented in Fig. 11.

Although the onset of chaos is observed due to a single parameter perturbation, the drawback of such an approach is that the associated perturbation amplitude has to be comparable to the parameter's equilibrium value ($\delta_\varepsilon = \delta_\xi = 0.4$). This is why we conducted additional analysis of complex dynamics of the model (3) by choosing a value of angular frequency admitting the periodic motion of the block in an unperturbed state, while the dynamics is observed by changing the perturbation amplitudes for each of the observed parameter separately (Fig. 13).

As it is clear from Fig. 13, in case of perturbing only a single parameter (ε or ξ), there is a direct transition to deterministic chaos for both amplitude values δ_ε and δ_ξ in the range [0,0.4]. This type of scenario to chaos could imply the existence of some global bifurcation. One should note that for $\delta_\xi > 0.4$, system (3) becomes extremely stiff in the plausible parameter domains, meaning that an exceedingly small iteration step ($<10^{-5}$) is required to carry out the numerical integration.

In the next step of our analysis, we examined another case of a single amplitude perturbation, only this time with higher frequency values ($\omega_\varepsilon = \omega_\xi = 0.9$). As it can be seen in Fig. 14, for the higher frequency values, a transition from periodic motion to deterministic chaos is observed, which is a type of dynamics already captured in Fig. 6. By comparing orbital diagrams in Figs. 13 and 14, it is clear that the onset of chaos could be controlled only by tuning the angular frequencies of assumed periodic perturbation of the selected parameters (ε or ξ).

We further proceed by analyzing what occurs if both ε and ξ undergo small oscillations. As a first step in the analysis, we choose values of angular frequencies admitting the periodic motion of the block in an unperturbed state and observe the dynamics of the model (3) by simultaneously changing the amplitude values for both parameters ε and ξ (Fig. 15).

In this case, a transition from periodic motion to deterministic chaos is observed (Fig. 16), with the onset of chaos for higher perturbation amplitudes in comparison to Figs. 13 and 14. The conclusions on the character of the observed behavior rely on the two commensurate frequencies and well-developed continuous noise in the power spectrum for the time series $V(t)$, provided in Figs. 17(*1*) and 17(*2*), respectively.

Deterministic chaos is further corroborated by calculating the positive value of the maximal Lyapunov exponent, as indicated in Fig. 18, using two different methods [37,38].

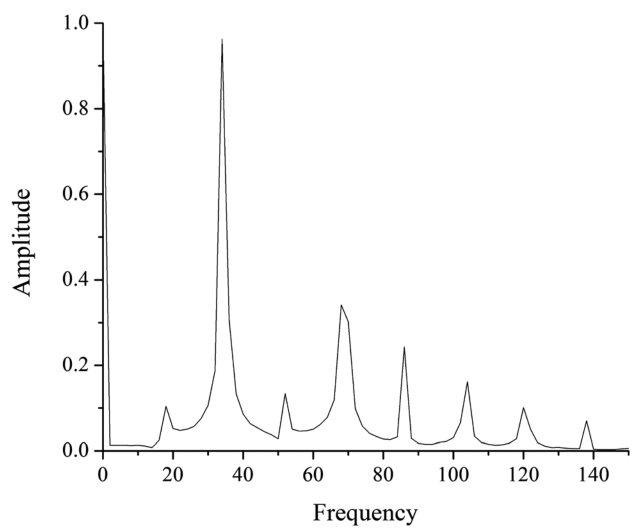

Fig. 12 Several incommensurate frequencies in Fourier power spectrum indicate quasi-periodic motion. Parameter values are the same as in Fig. 11.

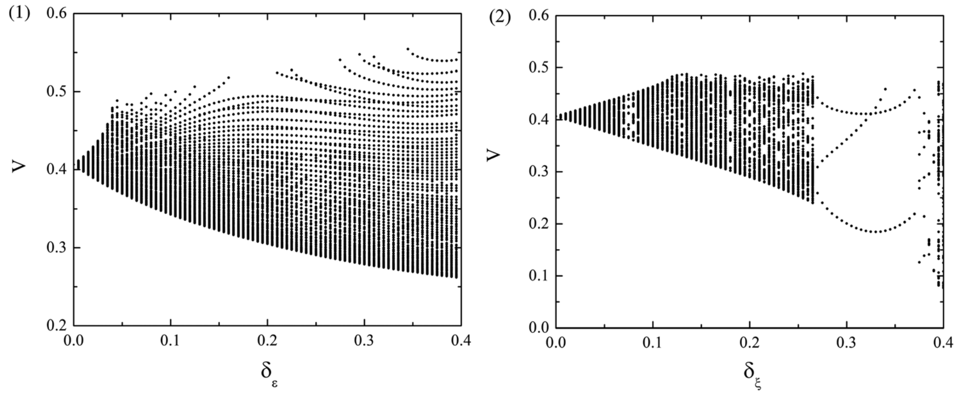

Fig. 13 Bifurcations of the system (4), for different perturbation amplitudes δ_ε and δ_ξ: (*1*) $\omega_\varepsilon = 0.2$; (*2*) $\omega_\xi = 0.3$. In both cases, orbital diagram is constructed for the section with plane $\theta = 1$, and calculation step $\omega_\varepsilon = \omega_\xi = 0.01$, showing the dynamics after 8×10^6 and 4×10^6 time units, respectively. At each instance, the parameters held constant are awarded values near the equilibrium point, but admitting the limit cycle, $\varepsilon = 0.4$, $\xi = 0.5$, and $\gamma = 0.8$.

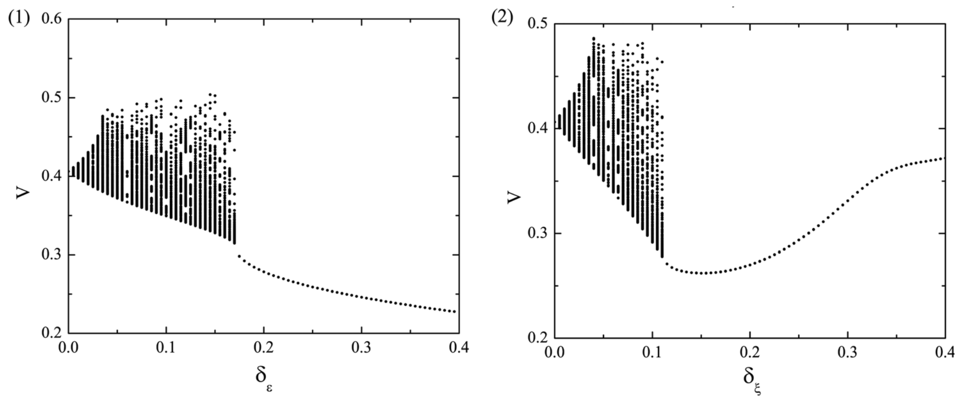

Fig. 14 Bifurcations of the system (3), for different perturbation amplitudes δ_ε and δ_ξ: (*1*) $\omega_\varepsilon = 0.9$; (*2*) $\omega_\xi = 0.9$. In both cases, orbital diagram is constructed for the section with plane $\theta = 1$, and calculation step $\omega_\varepsilon = \omega_\xi = 0.01$ showing the dynamics after 8×10^6 time units. At each instance, the parameters held constant are awarded values near the equilibrium point but admitting the limit cycle, $\varepsilon = 0.4$, $\xi = 0.5$, and $\gamma = 0.8$.

If we proceed with further analysis, this time by assuming high constant perturbation frequencies ($\omega_\varepsilon = \omega_\xi = 0.9$) and by simultaneously changing the amplitude values for both parameters ε and ξ, in the range [0,0.4], the system (3) exhibits only the periodic motion.

5 Concluding Remarks

In this paper, we analyze the effect of periodic parameter perturbation on the onset of complex dynamics in Burridge–Knopoff single-block model. In the first phase of the research, we examine the impact of a single parameter perturbation (ε or ξ) on the system's dynamics. The results indicate that the complex dynamics are observed only under a single parameter perturbation for limit amplitude values, with transition from periodic and quasi-periodic motion to deterministic chaos, interspersed with periodic and quasi-periodic windows between chaotic clouds of dots. An interesting finding is that the onset of chaos is observed for the frequencies of a single parameter perturbation near the frequency of periodic motion of the block in an unperturbed state ($\omega_\varepsilon = 0.2$, $\omega_\xi = 0.3$). In an earthquake analogy, it means that the instability of motion along the fault could be generated by small-amplitude oscillations with a frequency value admitting the aseismic motion along the fault. Further analysis of the system's dynamics with oscillation frequencies assumed constant

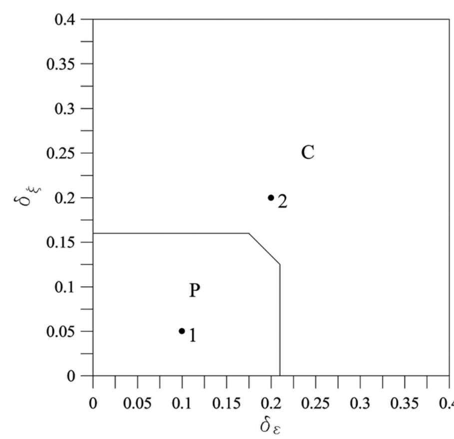

Fig. 15 Attractors of the system (3) in parameter plane δ_ε - δ_ξ, for the frequencies near the frequency of the block in unperturbed state, admitting chaos due to a single parameter perturbation ($\omega_\varepsilon = 0.2$, $\omega_\xi = 0.3$). Diagram is constructed for the grid 0.01×0.01. At each instance, the parameters held constant are awarded the values near the equilibrium point but admitting the limit cycle, $\varepsilon = 0.4$, $\xi = 0.5$, and $\gamma = 0.8$. P and C are abbreviations for periodic motion and deterministic chaos, respectively. Corresponding time series and phase portraits for points 1 and 2 are shown in Fig. 16.

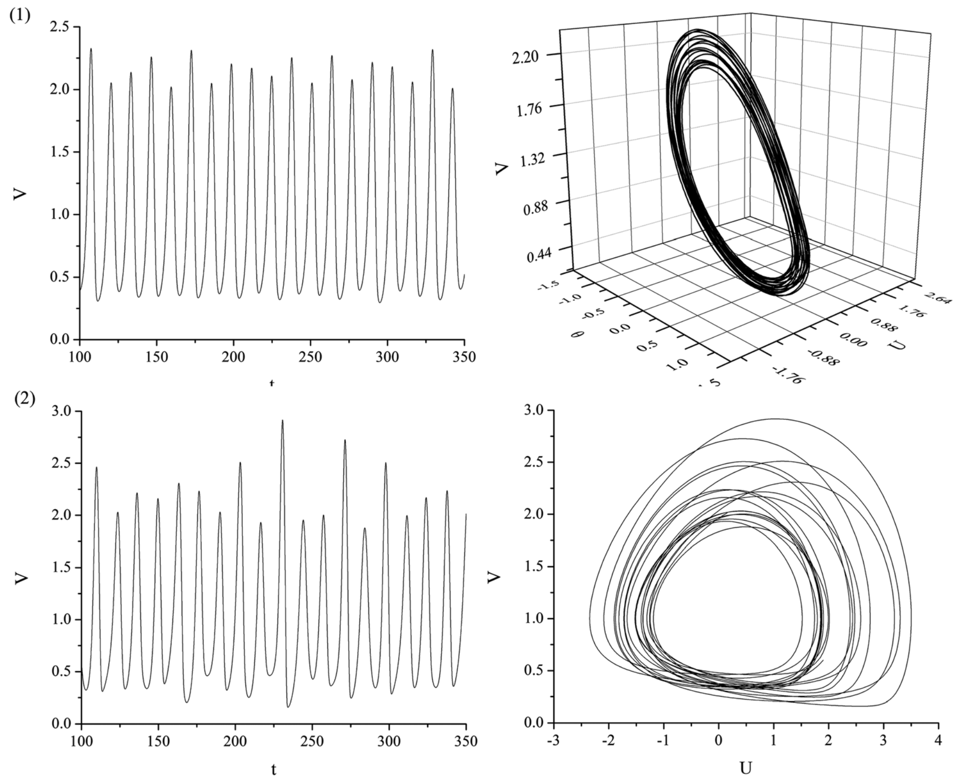

Fig. 16 Temporal evolution of variable *V* and the appropriate phase portraits for points 1 and 2 in Fig. 15: (*1*) $\delta_\varepsilon = 0.1$, $\delta_\xi = 0.05$ (periodic motion); (*2*) $\delta_\varepsilon = 0.2$, $\delta_\xi = 0.2$ (deterministic chaos). At each instance, the parameters held constant are awarded values near the equilibrium point but admitting the limit cycle, $\varepsilon = 0.4$, $\xi = 0.5$, and $\gamma = 0.8$. Values of the angular frequency are chosen to be near the angular frequency of the block in an unperturbed state, admitting the onset of deterministic chaos for a single parameter perturbation: $\omega_\varepsilon = 0.2$, $\omega_\xi = 0.3$.

($\omega_\varepsilon = 0.2$, $\omega_\xi = 0.3$) and only by changing the perturbation amplitudes δ_ε and δ_ξ in the range [0,0.4] shows a direct transition to deterministic chaos, which could indicate the existence of global bifurcations. On the other hand, for higher oscillation frequencies ($\omega_\varepsilon = \omega_\xi = 0.9$), a transition from periodic motion to deterministic chaos is observed. In this case, it is obvious that the onset of chaos could be controlled only by tuning the angular frequencies of assumed single parameter perturbation.

In the second phase of the research, we assume the coaction of both parameters ε and ξ. By changing only the perturbation amplitudes of both parameters in the range [0,0.4] with constant values of frequencies admitting the periodic motion of the block in an unperturbed state ($\omega_\varepsilon = 0.2$, $\omega_\xi = 0.3$), the results indicate the transition from periodic motion to deterministic chaos, with the onset of chaos only for higher values of perturbation amplitudes in comparison to the case when only a single parameter is perturbed. On the other side, the system (3) exhibits only the periodic motion for the coaction of both perturbed parameters if higher frequency values are presumed ($\omega_\varepsilon = \omega_\xi = 0.9$).

It has to be emphasized that sinusoidal oscillations represent an idealistic case of parameter perturbation, which rarely occurs

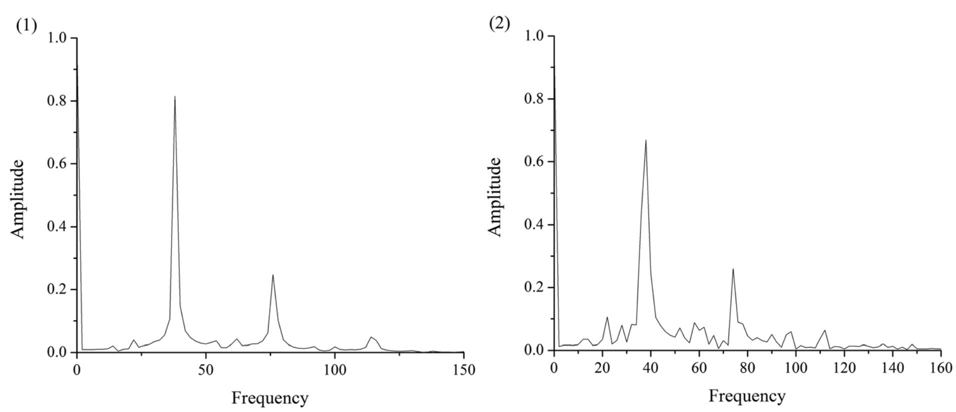

Fig. 17 (*1*) Two commensurate peaks in power spectrum (first peak for the fundamental frequency, and the second peak for the harmonic) imply the periodic motion (*2*). The broadband noise in the Fourier power spectrum indicates the chaotic behavior of the system. The parameter values are the same as in Figs. 16(*1*) and 16(*2*), respectively.

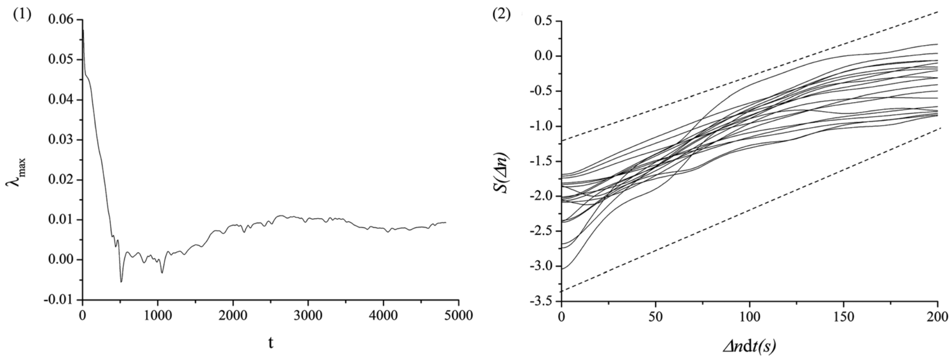

Fig. 18 Calculation of maximal Lyapunov exponent for a time series in Fig. 17(*2*): (*1*) $\lambda_{max} = 0.009$ (method of Wolf et al. [37]); (*2*) $\lambda_{max} \approx 0.009$ (method of Rosenstein et al. [38]). Effective expansion rate $S(\Delta n)$ represents the average of the logarithm of $D_i(\Delta n)$, defined as the average distance of all nearby trajectories to the reference trajectory as a function of the relative time Δn. The slope of dashed lines indicating the predominant slope of $S(\Delta n)$ in dependence on $\Delta n dt$ presents a robust estimate for the maximal Lyapunov exponent. The results are determined for 1000 reference points and neighboring distance $\varepsilon = 0.1$–0.5.

under the real conditions in Earth's crust. However, as already stated in the introductory part, we believe they are of interest because of their simple shape and because a real wave pattern results in a superposition of such periodic waves. Also, some earthquakes that arise from slow rupture along the faults could generate seismic waves of such simple shape [33], or they could occur as a product of some artificial source (e.g., heavy mining machines and equipment).

Nevertheless, though the analyzed model and the assumed perturbations are rather simple, the performed analysis showed that the onset of deterministic chaos could be observed for small values of the control parameter ε, which is in contrast to the research conducted by Erickson et al. [20], who observed the occurrence of deterministic chaos in Burridge–Knopoff single-block model for $\varepsilon = 11$. On the other side, the results of our analysis correspond well with the research also conducted by Erickson et al. [39], where the transition to chaos is observed for $\varepsilon = 0.5$ as the number of blocks increases from 20 to 21. This further implies that the onset of chaos does not have to be size dependent, as it was already indicated in our previous research on the dynamics of spring-block model with time delay [27].

In the present paper, the focus has been on introducing a minimal model of fault dynamics that can exhibit chaotic behavior. The possible gain from such an approach lies in highlighting the more subtle mechanisms otherwise neglected in the models that involve the compound fault structure. What we actually suggest is that the results obtained here should be viewed as complementary to those established for the more complex models. Nonetheless, the strategy we adopted can likely be replicated in case of the larger number of blocks or be incorporated into the model of a transform fault, implying that the current results may further be reevaluated under some more realistic setups.

Acknowledgment

This research has been supported by the Ministry of Education, Science and Technological Development of the Republic of Serbia, Contract Nos. 176016, 171015, and 171017.

References

[1] Ohnaka, M., 1993, "Critical Size of the Nucleation Zone of Earthquake Rupture Inferred From Immediate Foreshock Activity," J. Phys. Earth, **41**, pp. 45– 56.
[2] Ellsworth, W. L., and Beroza, G. C., 1995, "Seismic Evidence for an Earthquake Nucleation Phase," Science, **268**, pp. 851–855.
[3] Dodge, D. A., Beroza, G. C., and Ellsworth, W. L., 1996, "Detailed Observations of California Foreshock Sequences: Implications for the Earthquake Initiation Process," J. Geophys. Res., **101**, pp. 22,371–22,392.
[4] Abercrombie, R., and Mori, J., 1994, "Local Observations of the Onset of a Large Earthquake: 28 June 1992 Landers, California," B. Seismol. Soc. Am. **84**, pp. 725–734.
[5] Mori, J., and Kanamori, H., 1996, "Initial Rupture of Earthquakes in the 1995 Ridgecrest, California Sequence," Geophys. Res. Lett., **23**, pp. 2340–2437.
[6] Geller, R. J., 1976, "Body Force Equivalents for Stress-Drop Seismic Sources," B. Seismol. Soc. Am., **66**, pp. 1801–1804.
[7] Ben-Menahem, A., and Singh, S. J., 2000, *Seismic Waves and Sources*, Springer-Verlag, New York.
[8] Aki, K., and Richards, P. G., 2002, *Quantitative Seismology, Theory and Methods*, Freeman, San Francisco.
[9] Gibowicz, S. J., and Kijko, A., 1994, *An Introduction to Mining Seismology*, Academic Press, Salt Lake City, UT.
[10] Brace, W., and Byerlee, J., 1966, "Stick-Slip as a Mechanism for Earthquakes," Science, **153**(3739), pp. 990–992.
[11] Burridge, R., and Knopoff, L., 1967, "Model and Theoretical Seismicity," B. Seismol. Soc. Am. **57**, pp. 341–371.
[12] Carlson, J. M., and Langer, J. S., 1989, "Mechanical Model of an Earthquake Fault," Phys. Rev. A, **40**, pp. 6470–6484.
[13] Elmer, F.-J., 1997, "Self-Organized Criticality With Complex Scaling Exponents in the Train Model," Phys. Rev. E, **56**, pp. R6225–R6228.
[14] Galvanetto, U., 2002, "Some Remarks on the Two-Block Symmetric Burridge–Knopoff Model," Phys. Lett. A, **293**, pp. 251–259.
[15] Popp, K., and Stelter, P., 1990, "Stick-Slip Vibrations and Chaos," Phil. Trans. R. Soc. Lond. A, **332**, pp. 89–105.
[16] Galvanetto, U., 2001, "Some Discontinuous Bifurcations in a Two-Block Stick-Slip System," J. Sound Vib., **248**, pp. 653–669.
[17] Ranjith, K., and Rice, J. R., 1999, "Stability of Quasi-Static Slip in a Single Degree of Freedom Elastic System With Rate and State Dependent Friction," J. Mech. Phys. Solids, **47**, pp. 1207–1218.
[18] Scholz, C. H., 2002, *The Mechanics of Earthquakes and Faulting*, Cambridge University Press, Cambridge.
[19] Montagne, R., and Vasconcelos, G. L., 2004, "Complex Dynamics in a One-Block Model for Earthquakes," Physica A, **342**, pp. 178–185.
[20] Erickson, B., Birnir, B., and Lavallee, D., 2008, "A Model for Aperiodicity in Earthquakes," Nonlinear Proc. Geoph., **15**, pp. 1–12.
[21] Pomeau, Y., and Le Berre, M., 2011, "Critical Speed-Up vs Critical Slow-Down: A New Kind of Relaxation Oscillation With Application to Stick-Slip Phenomena," arXiv: 1107.3331v1.
[22] Ruina, A. L., 1983, "Slip Instability and State Variable Friction Laws," J. Geophys. Res., **88**, pp. 10359–10370.
[23] Tullis, T. E., and Weeks, J. D., 1986, "Constitutive Behavior and Stability of Frictional Sliding in Granite," Pure Appl. Geophys., **124**, pp. 383–414.
[24] Dieterich, J. H., 1979, "Modeling of Rock Friction, 1. Experimental Results and Constitutive Equations," J. Geophys. Res., **84**, pp. 2161–2168.
[25] Madariaga, R., and Olsen, K. B., 2002, "Earthquake Dynamics," *International Handbook of Earthquake and Engineering Seismology, Part A.*, W. H. K. Lee, H. Kanamori, P. C. Jennings, and C. Kisslinger, eds., Academic Press, London, pp. 176–194.
[26] Kawamura, H., Hatano, T., Kato, N., Biswas, S., and Chakrabarti, B. K., 2012, Statistical Physics of Fracture, Friction and Earthquake, Rev. Mod. Phys., **84**, pp. 839–884.
[27] Kostić, S., Franović, I., Todorović, K., and Vasović, N., 2013, "Friction Memory Effect in Complex Dynamics of Earthquake Model," Nonlinear Dynam., **73**(3), pp. 1933–1943.

[28] Gomberg, J., Blanpied, M., and Beeler, N., 1997, "Transient Triggering of Near and Distant Earthquakes," B. Seismol. Soc. Am., **87**, pp. 294–309.
[29] Perfettini, H., Schmittbuhl, J., and Cochard, A., 2003, "Shear and Normal Load Perturbations on a Two-Dimensional Continuous Fault: 2. Dynamic Triggering," J. Geophys. Res. **108**(2409), pp. 1–16.
[30] Burić, N., and Vasović, N., 1999, "A Simple Model of the Chaotic Immune Response," Chaos Soliton. Fract. **10**, pp. 1185–1192.
[31] Dieterich, J. H., and Kilgore, B. D., 1994, "Direct Observation of Frictional Contacts: New Insights for State Dependent properties," Pure Appl. Geophys., **143**, pp. 283–302.
[32] Rice, J. R., Lapusta, N., and Ranjith, K., 2001, "Rate and State Dependent Friction and the Stability of Sliding Between Elastically Deformable Solids," J. Mech. Phys. Solids, **49**, pp. 1865–1898.
[33] Gomberg, J., Bodin, P., Savage, W., and Jackson, M. E., 1995, "Landslide Faults and Tectonic Faults, Analogs?—The Slumgullion Earthflow, Colorado," Geology, **23**, pp. 41–44.
[34] Perfettini, H., Schmittbuhl, J., Rice, J. R., and Cocco, M. J., 2001, "Frictional Response Induced by Time-Dependent Fluctuations of the Normal Loading," Geophys. Res., **106**, pp. 13455–13472.
[35] Gomberg, J., Beeler, N. M., Blanpied, M. L., and Bodin, P., 1998, "Earthquake Triggering by Transient and Static Deformations," J. Geophys. Res., **103**, pp. 24411–24426.
[36] Parsons, T., 2005, "A Hypothesis for Delayed Dynamic Earthquake Triggering," Geophys. Res. Lett., **32**(4), pp. 1–4.
[37] Wolf, A., Swift, J., Swinney, H., and Vastano, J., 1985, "Determining Lyapunov Exponents From a Time Series," Physica D, **16**, pp. 285–317.
[38] Rosenstein, M. T., Collins, J. J., and De Luca, C. J., 1993, "A Practical Method for Calculating Largest Lyapunov Exponents From Small Data Sets," Physica D, **65**, pp. 117–134.
[39] Erickson, B. A., Birnir, B., and Lavallée, D., 2011, "Periodicity, Chaos and Localization in a Burridge–Knopoff Model of an Earthquake With Rate-and-State Friction," Geophys. J. Int., **187**, pp. 178–198.